Electronic Supplementary Material (ESI) for Inorganic Chemistry Frontiers.
This journal is © the Partner Organisations 2021

Electronic Supporting Information

EPR-derived structures of flavin radical and iron-sulfur cluster from

Methylosinus sporium 5 reductase

Han Sol Jeong,[ab†] Sugyeong Hong,[ab†] Hee Seon Yoo,[c] Jin Kim,[d] Yujeong Kim,[ab]

Chungwoon Yoon,[c] Seung Jae Lee[c*] and Sun Hee Kim[ab*]

[a]Western Seoul Center, Korea Basic Science Institute (KBSI), Seoul 03759, Rep. of Korea. E-mail: shkim7@kbsi.re.kr

[b]Department of Chemistry and Nano Science, Ewha Womans University, Seoul 03760, Republic of Korea.

[c]Department of Chemistry and Institute of Molecular Biology and Genetics, Jeonbuk National University, Jeonju 54896, Republic of Korea. E-mail: slee026@jbnu.ac.kr

[d]Department of Chemistry, Sunchon National University, Suncheon 57922, Republic of Korea

[†]These authors contributed equally to this work.

Supplementary Schemes

Scheme S1. Alignment of amino acids from ferredoxin domain of sMMO. Gray and red color represent identical and different amino acids, respectively.

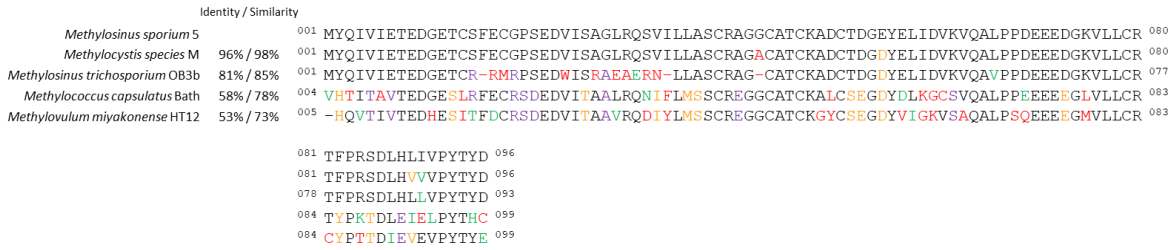

Scheme S2. Alignment of amino acids from FAD binding domain of sMMO. Gray and red color represent identical and different amino acids, respectively.

Scheme S3. The schematic drawing of three types of [2Fe-2S]+ clusters. (a) Ferredoxin, (b) MitoNEET, and (c) Rieske-type.

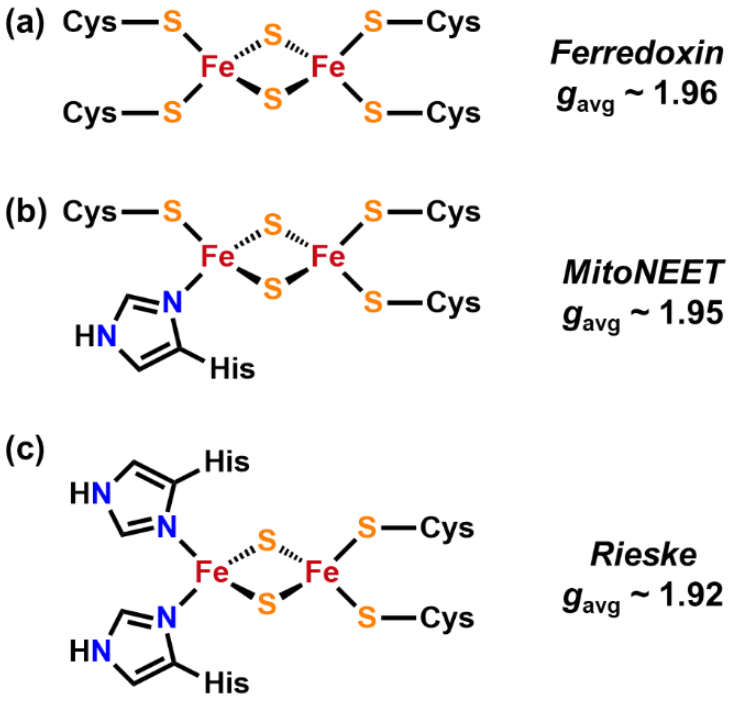

Scheme S4. Schematic representation of a proton positioned nearly from the Fe^{II} and Fe^{III} ions of the $[2Fe\text{-}2S]^+$ cluster.

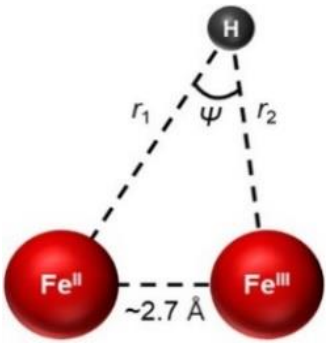

To estimate the position of the proton from the $[2Fe\text{-}2S]^+$ cluster, the dipolar hyperfine coupling value of A_{dip} is used by considering the spin projection factor of the respective nucleus. The spin projection factors of two metal atoms, p_A and p_B, are given as follows:

$$p_A = \frac{S(S+1) + S_A(S_A+1) - S_B(S_B+1)}{2S(S+1)}$$
$$p_B = \frac{S(S+1) - S_A(S_A+1) + S_B(S_B+1)}{2S(S+1)}$$

where S is total spin of the cluster, and S_A and S_B are the local spin of each metal atom.[S1,S2] The spin projection factors of Fe(II) ($S_A = 2$) and Fe(III) ($S_B = 5/2$) of the $[2Fe\text{-}2S]^+$ cluster are –4/3 (p_A) and +7/3 (p_B), respectively. Thus, A_{dip} can be calculated by equations as follows:

$$A_{dip} = c\left(-\delta, -\Gamma + \frac{\delta}{2}, \Gamma + \frac{\delta}{2}\right)$$
$$\delta = p_A r_1^{-3} + p_B r_2^{-3}$$
$$\Gamma = \frac{3}{2}\sqrt{p_A^2 r_1^{-6} + p_A p_B r_1^{-3} r_1^{-3} cos2\psi + p_B^2 r_2^{-6}}$$

where c is $g_e\mu_e g_n\mu_e$ and equals 79 MHz Å^3 for a proton, and geometrical parameters r and ψ are defined in **Scheme S3**.[S3,S4] From the equation, the distances between the iron ions and the exchangeable proton are estimated to be r_1 = 4.1-4.4 and r_2 =3.50-3.60 Å with ψ ~40°. The distance between the Fe^{II} and Fe^{III} centers can also be calculated in accordance with the law of cosines and was estimated to be ~2.7 Å.[S5]

Supplementary Tables

Table S1. The simulation parameters for ^{1}H Davies ENDOR spectra of the [2Fe-2S]$^{+}$ cluster.

	$A(^{1}H)$ (MHz)	[α, β, λ] (°)
Exchangeable proton	[6.15 ± 0.35, –3.50 ± 0.15, –2.90 ± 0.15]	[30, 90, 50]
Non-exchangeable proton	[2.32 ± 0.12, 11.70 ± 0.20, 1.58 ± 0.08]	[80, 30, 90]

Table S2. Simulation parameters for ^{14}N three-pulse ESEEM and HYSCORE spectra of the $[2Fe\text{-}2S]^{+}$ cluster.

	N_1	N_2
$A(^{14}N)$ (MHz)	[1.2, 1.2, 1.2]	[0.9, 0.6, 0.6]
$A_{iso}(^{14}N)$ (MHz)	1.2	0.7
e^2qQ/h (MHz)	3.4	3.0
η	0.4	0.9
[Q_α, Q_β, Q_λ] (°)	[–75, 100, 60]	[0, 90, 0]

Table S3. The reported hyperfine and quadrupole coupling parameters of ^{14}Ns coupled to the [2Fe-2S]$^{+}$ cluster.

	A_{iso} (MHz)	e^2qQ/h (MHz)	Refs.
Rieske or Rieske-type			
bc1 (bovine)	3.55	2.25	S6
	5.20	2.93	
bc1 (bovine) + UHDBT	3.40	2.30-2.65	
	5.30	2.60-3.00	
Cytochrome b6f (spinach)	4.58	2.70	S7
	3.75	2.70	
Burkholderia cepacia	3.70	2.15	S8
	4.70	3.85	
B. cepacia AC 1100	3.87	2.40	S9
	4.90	2.32	
Pseudomonas putida	3.56	2.43	S10
	4.78	2.31	
Pseudomonas cepacia	4.28	2.60	S9
	5.49	2.30	
2,4,5-Trichlorophenoxyacetate Monooxygenase	3.40	2.36	S11
	5.10	2.52	
Ferredoxin or ferredoxin-type			
P. putida	1.11	3.27	S10
Clostridum pasteurianum	0.61	3.29	S12
Arum maculatum	1.10	3.32	S6
Spirulina platensis	1.01	3.52	S6
E. coli (reduced)	1.06	3.41	S6
E. coli (oxidized)	1.10	3.30	S13
Porphyra umbilicalis	1.16	3.24	S14
	0.40	3.04	
Yarrowia lipolytica	0.90	3.10	S15
Adrenodoxin	1.05	3.10	S16
	0.65	2.90	
Arthrospira plantensis ferredoxin	1.16	3.10	
	0.72	2.90	

Table S4. Cartesian coordinates for the optimized geometries.

(a) Neutral flavin radical

N	-2.414300	-0.002840	-0.350910
C	-3.462390	-0.897250	-0.246360
O	-4.627580	-0.565660	-0.307690
N	-3.138700	-2.262240	-0.051520
C	-1.874220	-2.791590	0.086793
O	-1.632360	-3.978330	0.277746
C	-0.837230	-1.785230	-0.022260
N	0.456424	-2.186840	0.095316
C	1.504528	-1.294860	0.027977
C	2.828325	-1.711820	0.191791
C	3.887589	-0.817000	0.124517
C	5.303507	-1.301680	0.305671
C	3.605500	0.547178	-0.111610
C	4.717485	1.562933	-0.185910
C	2.283268	0.960011	-0.273760
C	1.208267	0.066410	-0.215640
N	-0.127170	0.473334	-0.397930
C	-1.171850	-0.432620	-0.255420
C	-0.439600	1.848180	-0.819620
C	-0.571960	2.888741	0.313996
O	-0.743920	4.156021	-0.303730
C	-1.747170	2.618377	1.259150
O	-2.972070	2.721223	0.552885
H	-1.750510	3.397190	2.026123
H	-1.641730	1.648105	1.758025
H	-1.694010	4.220592	-0.481240
H	0.356189	2.936861	0.893044
H	-1.381320	1.807795	-1.363370
H	0.331908	2.182590	-1.512290
H	4.326743	2.563902	-0.372580
H	5.424233	1.324163	-0.987180
H	5.292986	1.596094	0.744891
H	5.331793	-2.378230	0.479685
H	5.916107	-1.088840	-0.576160
H	5.789284	-0.812210	1.155769
H	2.093608	2.010381	-0.442460
H	3.018837	-2.764480	0.374478
H	0.599304	-3.178510	0.258702
H	-3.923420	-2.896660	0.021065
H	-3.120640	1.856585	0.129258

(b) Anionic flavin radical

N	-2.393210	0.005143	-0.330220
C	-3.448690	-0.864050	-0.246410
O	-4.622990	-0.512970	-0.312350
N	-3.136460	-2.216060	-0.069330
C	-1.870250	-2.794930	0.079038
O	-1.761710	-4.001410	0.255585
C	-0.783340	-1.820840	-0.010800
N	0.493493	-2.261470	0.116041
C	1.470644	-1.329430	0.038786
C	2.819761	-1.727500	0.190895
C	3.885654	-0.841370	0.122710
C	5.300808	-1.342940	0.294573
C	3.623364	0.525053	-0.105480
C	4.742748	1.535137	-0.182030
C	2.294739	0.946729	-0.259690
C	1.221315	0.057218	-0.199190
N	-0.113000	0.461644	-0.372360
C	-1.147640	-0.470040	-0.234840
C	-0.425130	1.816773	-0.823720
C	-0.560970	2.884238	0.281675
O	-0.825780	4.136787	-0.353690
C	-1.690840	2.586511	1.271689
O	-2.940450	2.625999	0.602347
H	-1.700620	3.376591	2.029453
H	-1.529180	1.625828	1.773354
H	-1.782440	4.114978	-0.507490
H	0.383766	2.994508	0.823344
H	-1.369170	1.768735	-1.363740
H	0.347130	2.142130	-1.523370
H	4.351766	2.538702	-0.364540
H	5.450330	1.305212	-0.988450
H	5.328536	1.573263	0.744996
H	5.310111	-2.421890	0.461970
H	5.918142	-1.136970	-0.588030
H	5.802444	-0.868950	1.146720
H	2.112575	2.001270	-0.423490
H	2.984989	-2.785440	0.364386
H	-3.921760	-2.848300	-0.004520
H	-3.028010	1.744914	0.171956

Supplementary Figures

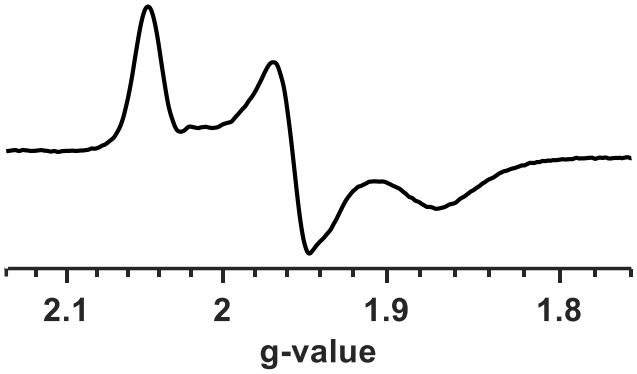

Fig. S1 X-band CW-EPR spectrum of the reduced MMOR after addition of $Na_2S_2O_4$ measured at 35 K. The experimental conditions: microwave frequency = 9.64 GHz, microwave power = 1 mW, modulation amplitude = 10 G, modulation frequency = 100 kHz, time constant = 40.96 ms.

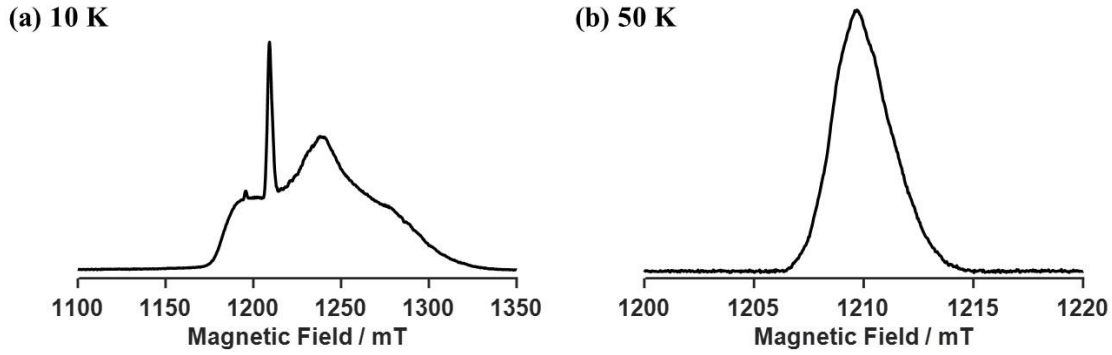

Fig. S2 Q-band ESE spectra of reduced MMOR at different temperatures. The experimental conditions: microwave frequency = 33.9 GHz, microwave power = 10 dB, pulse sequence = $\pi/2$(32 ns) -τ-π (64 ns), τ = 300 ns, temperature = (a) 10 K, (b) 50 K.

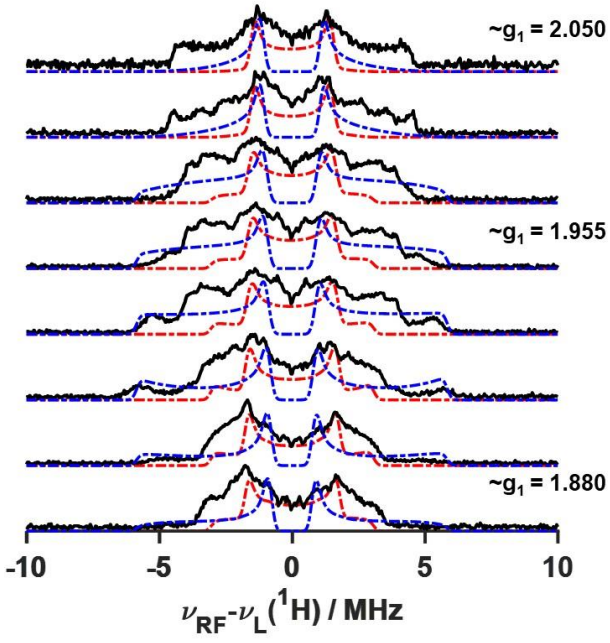

Figure S3. Q-band ^{1}H Davies ENDOR of $[2Fe\text{-}2S]^{+}$ cluster in MMOR (black line) and simulated spectra (dashed red line: exchangeable proton, dashed blue line: non-exchangeable proton). The simulation parameters are shown in table S1. The experimental conditions: microwave frequency = 33.9 GHz, $\pi/2$ = 32 ns, τ = 300 ns, RF length = 20 μs, temperature = 10 K.

(a)

Methylosinus sporium 5	^{39}S**C**RAGG**C**AT**C**…L^{80}**C**R
Anthrospira platensis	^{40}S**C**RAGA**C**ST**C**…T^{79}**C**V

(b)

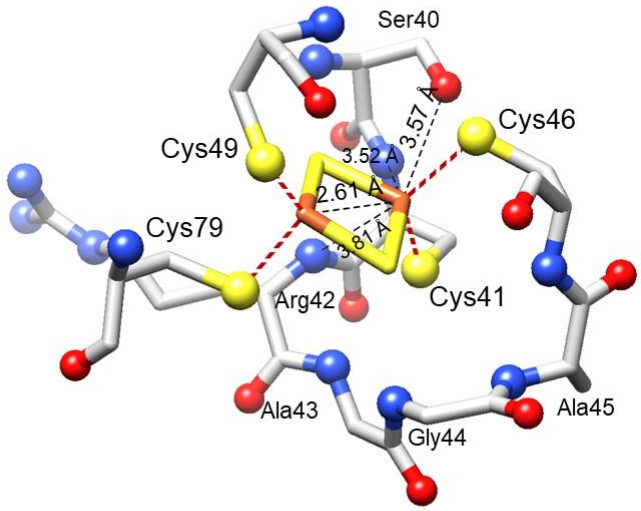

Arthrospira platensis

PDB ID: 4FXC

Figure S4. (a) Amino acid sequences of residues located around the [2Fe-2S]$^{+}$ cluster of *Methylosinus sporium 5* and *Anthrospira platensis*, and the immediate environment of the [2Fe-2S]$^{+}$ cluster of the ferredoxin of (b) *Anthrospira platensis* with selected bond distances of Fe–Fe and proximal H…Fe. Note that the positions of protons in the ferrodoxin domain of *Anthrospira platensis* were not well resolved by X-ray crystallography. Color code: orange, Fe; yellow, S; red, O; blue, N; gray, C; white, H.

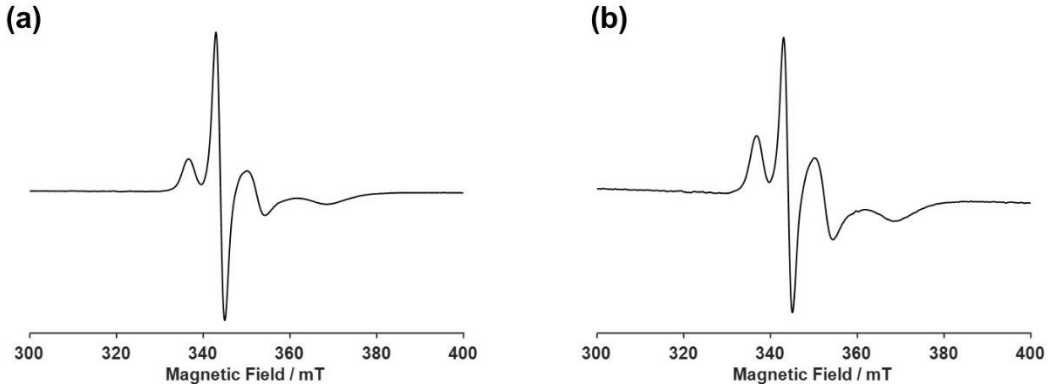

Figure S5. CW-EPR spectra of MMOR (a) and MMOR+MMOB (b). The experimental conditions: microwave frequency = 9.64 GHz, microwave power = 1 mW, modulation amplitude = 10 G, modulation frequency = 100 kHz, time constant = 40.96 ms, temperature = 35 K.

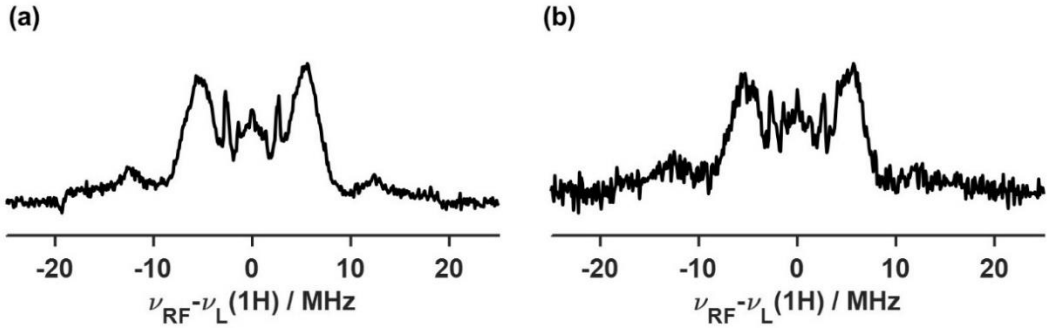

Figure S6. 34 GHz ^{1}H Davies ENDOR of neutral flavin radical species in (a) MMOR and (b) MMOR+MMOB. The experimental conditions: microwave frequency = 33.9 GHz, Pulse sequence = 64 ns-32 ns-64 ns (π-π/2-π), τ = 300 ns, RF length = 20 μs, temperature = 50 K.

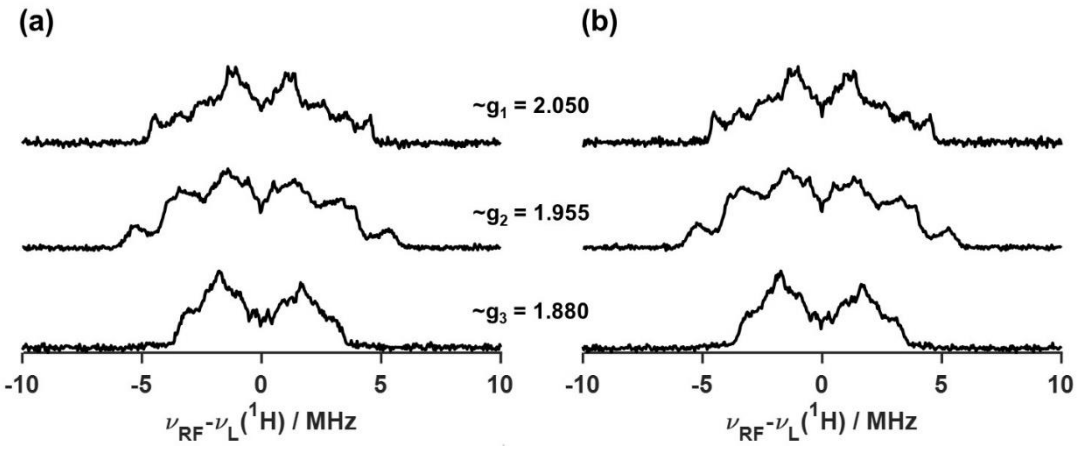

Figure S7. 34 GHz ^{1}H Davies-ENDOR of $[2Fe\text{-}2S]^{+}$ cluster in (a) MMOR and (b) MMOR+MMOB. The experimental conditions: microwave frequency = 33.9 GHz, π = 64 ns, $\pi/2$ = 32 ns, τ = 300 ns, RF length = 20 μs, temperature = 10 K.

References

(S1) A. Bencini and D. Gatteschi, Electron paramagnetic resonance of exchange coupled systems, *Springer Verlag: Berlin*, 1990.

(S2) M.-E. Pandelia, N. D. Lanz, S. J. Booker and C. Krebs, Mössbauer spectroscopy of Fe/S proteins, *Biochim. Biophys. Acta*, 2015, **1853**, 1395-1405.

(S3) R. Fiege, W. Zweygart, R. Bittl, N. Adir, G. Renger and W. Lubitz, EPR and ENDOR studies of the water oxidizing complex of Photosystem II, *Photosynth. Res.*, 1996, **48**, 227-237.

(S4) D. W. Randall, A. Gelasco, M. T. Caudle, V. L. Pecoraro and R. D. Britt, ESE-ENDOR and ESEEM characterization of water and methanol ligation to a dinuclear Mn(III)Mn(IV) complex, *J. Am. Chem. Soc.*, 1997, **119**, 4481-4491.

(S5) J. Müller, A. A. Lugovskoy, G. Wagner and S. J. Lippard, NMR structure of the [2Fe-2S] ferredoxin domain from soluble methane monooxygenase reductase and interaction with its hydroxylase, *Biochemistry*, 2002, **41**, 42-51.

(S6) J. K. Shergill and R. Cammack, ESEEM and ENDOR studies of the Rieske iron-sulphur protein in bovine heart miochondrial membranes, *Biochim. Biophys. Acta*, 1994, **1185**, 35-42.

(S7) R. D. Britt. K. Sauer and M. P. Klein, Electron spin echo envelope modulation spectroscopy supports the suggested coordination of two histidine ligands to the Rieske Fe-S centers of the cytochrome b_0f complex of spinach and the cytochrome bc_1 complexes of *Rhodospirillum rubrum*, *Rhodobacter sphaeroides* R-26, and bovine heart mitochondria, *Biochemistry*, 1991, **30**, 1892-1901.

(S8) A. Riedel, S. Fetzner, M. Rampp, F. Lingens, U. Liebl, J. Zimmermann and W. Nitschke, EPR, electron spin echo envelope modulation, and electron nuclear double resonance studies of the 2Fe-2S centers of the 2-halobenzoate 1,2-dioxygenase from *Burkholderia* (*Pseudomonas*) *cepacia* 2CBS, *J. Biol. Chem.*, 1995, **270**, 30869-30873.

(S9) R. J. Gurbiel, C. J. Batie, M. Sivaraja, A. E. True, J. A. Fee, B. M. Hoffman and D. P. Ballou, Electron-nuclear double resonance spectroscopy of ^{15}N-enriched phthalate dioxygenase from *Pseudomonas cepacia* proves that two histidines are coordinated to the [2Fe-2S] Rieske-type clusters, *Biochemistry*, 1989, **28**, 4861-4871.

(S10) J. K. Shergill, C. L. Joannou, J. R. Mason and R. Cammack, Coordination of the Rieske-type [2Fe-2S] cluster of the terminal iron—sulfur protein of *Pseudomonas putida* benzene 1,2-dioxygenase, studied by one- and two-dimensional electron spin-echo envelope modulation spectroscopy, *Biochemistry*, 1995, **34**, 16533-16542.

(S11) S. A. Dikanov, R. M. Davydov, L. Xun and M. K. Bowman, CW and pulsed EPR characterization of the reduction of the Rieske-Type iron–sulfur cluster in 2,4,5-trichlorophenoxyacetate monooxygenase, *J. Magn. Reson.*, 1996, **112**, 289-294.

(S12) J. K. Shergill, M. Golinelli, R. Cammack and J. Meyer, Coordination of the [2Fe-2S] cluster in wild type and molecular variants of *Clostridium pasteurianum* ferredoxin, investigated by ESEEM spectroscopy, *Biochemistry*, 1996, **35**, 12842-12848.

(S13) R. Cammack and A. Chapman, Electron spin-echo spectroscopy of the iron-sulphur clusters of xanthine oxidase from milk, *J. Chem. Soc. Faraday Trans*, 1991, **87**, 3203-3206.

(S14) S. A. Dikanov, A. M. Tyryshkin, I. Felli, E. J. Reuerse and J. Hüttermann, C-Band ESEEM of strongly coupled peptide nitrogens in reduced two-iron ferredoxin, *J. Magn. Reson.*, 1995, **108**, 99-102.

(S15) T. Maly, L. Gregic, K. Zwicker, V. Zickermann, U. Brandt and T. Prisner, Cluster N1 of complex I from *Yarrowia lipolytica* studied by pulsed EPR spectroscopy, *J. Biol. Inorg. Chem.*, 2006, **11**, 343-350.

(S16) S. A. Dikanov, R. I. Samoilova, R. Kappl, A. R. Crofts and J. Hüttermann, The reduced [2Fe-2S] clusters in adrenodoxin and *Arthrospira platensis* ferredoxin share spin density with protein nitrogens, probed using 2D ESEEM, *Phys. Chem. Chem. Phys.*, 2009, **11**, 6807-6819.